Published in final edited form as:
Int J Radiat Oncol Biol Phys. 2008 January 1; 70(1): 235–242. doi:10.1016/j.ijrobp.2007.08.036.

Reproducibility of Intratumor Distribution of ^{18}F-fluoromisonidazole in Head and Neck Cancer

Sadek A. Nehmeh, Ph.D.[*], **Nancy Y. Lee, M.D.**[†], **Heiko Schröder, M.D.**[‡], **Olivia Squire, R.N.**[‡], **Pat B. Zanzonico, Ph.D.**[*], **Yusuf E. Erdi, Ph.D.**[*], **Carlo Greco, M.D.**[†], **Gig Mageras, Ph.D.**[*], **Hai S. Pham, M.S.**[*], **Steve M. Larson, M.D.**[†], **Clifton C. Ling, Ph.D.**[*], and **John L. Humm, Ph.D.**[*]

[*]Department of Medical Physics, Memorial Sloan-Kettering Cancer Center, New York, NY

[†]Department of Radiation Oncology, Memorial Sloan-Kettering Cancer Center, New York, NY

[‡]Department of Radiology, Memorial Sloan-Kettering Cancer Center, New York, NY

Abstract

Purpose—Hypoxia is one of the main causes of the failure to achieve local control using radiotherapy. This is due to the increased radioresistance of hypoxic cells. ^{18}F-fluoromisonidazole (^{18}F-FMISO) positron emission tomography (PET) is a noninvasive imaging technique that can assist in the identification of intratumor regions of hypoxia. The aim of this study was to evaluate the reproducibility of ^{18}F-FMISO intratumor distribution using two pretreatment PET scans.

Methods and Materials—We enrolled 20 head and neck cancer patients in this study. Of these, 6 were excluded from the analysis for technical reasons. All patients underwent an ^{18}F-fluorodeoxyglucose study, followed by two ^{18}F-FMISO studies 3 days apart. The hypoxic volumes were delineated according to a tumor/blood ratio ≥1.2. The ^{18}F-FMISO tracer distributions from the two ^{18}F-FMISO studies were co-registered on a voxel-by-voxel basis using the computed tomography images from the PET/computed tomography examinations. A correlation between the ^{18}F-FMISO intensities of the corresponding spatial voxels was derived.

Results—A voxel-by-voxel analysis of the ^{18}F-FMISO distributions in the entire tumor volume showed a strong correlation in 71% of the patients. Restraining the correlation to putatively hypoxic zones reduced the number of patients exhibiting a strong correlation to 46%.

Conclusion—Variability in spatial uptake can occur between repeat ^{18}F-FMISO PET scans in patients with head and neck cancer. Blood data for one patient was not available. Of 13 patients, 6 had well-correlated intratumor distributions of ^{18}F-FMISO—suggestive of chronic hypoxia. More work is required to identify the underlying causes of changes in intratumor distribution before single-time-point ^{18}F-FMISO PET images can be used as the basis of hypoxia-targeting intensity-modulated radiotherapy.

Keywords

^{18}F-fluoromisonidazole; ^{18}F-FMISO; Hypoxia; Head and neck cancer

Reprint requests to: Sadek A. Nehmeh, Ph.D., Department of Medical Physics, Memorial Sloan-Kettering Cancer Center, 1275 York Ave., New York, NY 10021. Tel: (212) 639-2175; Fax: (917) 432-2379; nehmehs@mskcc.org.

Conflict of interest: none.

Introduction

Most solid tumors show evidence of hypoxia, presumably as a consequence of tumor cell proliferation outpacing neoangiogenesis (1–3). To date, three methods have been used to assess hypoxia in human tumors. These include direct interstitial measurement of the partial oxygen pressure (pO_2) using a polarographic oxygen electrode (Eppendorf GMbH, Hamburg, Germany). In a study of 28 head and neck cancer patients, Brizel *et al.* (4) showed that the average pretreatment median pO_2 was 11.2 mm Hg (range, 0.4–60 mm Hg), with a lower median pO_2 correlating with shorter disease-free survival. A more recent study (5) of 397 head and neck cancer patients from seven centers showed that a hypoxic fraction defined by a pO_2 <2.5 mm Hg threshold was associated with poor overall survival (Kaplan-Meier analysis, $p = 0.006$).

Although often considered the benchmark standard, pO_2 probe measurements are associated with the following disadvantages: invasiveness; limitation in sampling, because they are restricted to accessible access sites; and an inability to distinguish between hypoxic and necrotic tissue.

The second approach is based on immunohistochemical analyses of either endogenous hypoxia-related proteins or exogenously administered hypoxic cell markers. Koukourakis *et al.* (6) studied the relationship between the intensity of hypoxia-inducible factor 2α and carbonic anhydrase 9 staining in head and neck cancer patients undergoing radiotherapy (RT) and observed a significant inverse association with poor locoregional control ($p < 0.0001$ and $p = 0.0002$, respectively) and poor survival ($p = 0.0004$ and 0.002, respectively). The predictive value of endogenous, as well as exogenous, hypoxia markers for treatment outcome has been reviewed by Bussink *et al.* (7).

The third approach is based on a noninvasive imaging technique. Previous positron emission tomography (PET) studies using fluorine-18 labeled misonidazole (^{18}F-FMISO) (8) have demonstrated variable, but significant, levels of hypoxia in soft-tissue sarcomas (4,9–11), breast cancer (12,13), glioblastoma (14), and cancer of the uterine cervix (10,15). In head and neck cancer, evidence of hypoxia was found in 40% of cases (16,17).

Rajendran *et al.* (18) showed the feasibility of this approach using ^{18}F-FMISO PET to detect tissue hypoxia (corresponding to pO_2 values of ≤3 mm Hg) in imaging studies and showed that ^{18}F-FMISO uptake was directly related to tissue hypoxia (19). Different tumor/blood and tumor/muscle threshold ratios have been proposed as quantitative criteria for delineating hypoxic tumor volumes (19–23). To our knowledge, no standard PET criterion for defining hypoxia has yet been established. In the present study, we elected to adopt the criterion suggested by Rajendran *et al.* (19), using a tumor/blood ratio of ≥1.2 to define the hypoxic volumes, because our experience confirmed that in all patients <95% of the nontumor voxels were hypoxic using this criterion.

The effectiveness of local control in RT for head-and-neck cancer can be compromised by the presence of viable hypoxic cells in the target volume (11,24). Previous studies have shown that threefold greater radiation doses are required to achieve the same level of cell kill of hypoxic vs. normoxic cells (25–27). One potential strategy to improve the effectiveness of RT is to selectively boost the hypoxic volume within the tumor using intensity-modulated RT (IMRT) (28,29). In this approach, IMRT is used to increase the dose to the “hypoxic tumor volume,” a subvolume defined within the conventional gross tumor volume, as defined by the tumor hypoxia images (*e.g.*, ^{18}F-FMISO-PET). However, such a strategy is predicated on the time invariance of tumor hypoxia as detected by PET tracers. Thus, in this study, we investigated the reproducibility of the ^{18}F-FMISO distribution in patients with head-and-neck tumors by performing two PET studies 3 days apart for each patient before RT. The degree of correlation

between the distributions of ^{18}F-FMISO hypoxic target volumes from the sequential ^{18}F-FMISO studies was the principal focus of this work.

For simplicity, we have referred to ^{18}F-FMISO as FMISO for the rest of this report.

Methods and Materials

Patient data

We included 20 male head-and-neck cancer patients scheduled for definitive RT in this study. The Memorial Sloan-Kettering Cancer Center institutional review board (IRB No. 04-070) approved the study, and all patients provided written informed consent.

All patients underwent a pretherapy fluorodeoxyglucose (FDG)-PET/computed tomography (CT) scan on Day 0 and FMISO-PET/CT scans on Day 1 (FMISO1) and Day 4 (FMISO2). Only 14 patients were included in the analysis. Of the remaining 6, 2 did not show uptake in either FMISO scan, 1 showed no uptake in the second FMISO scan, and 3 were excluded for technical reasons. The average age of the 14 included patients was 58 years (range, 46–79). In one study (Patient 1), the blood sample coagulated; therefore, correlation between FMISO1 and FMISO2 voxels satisfying a tumor/blood (T/B) ratio $\geq$1.2 was not performed. Patient age, primary disease site, and disease stage are summarized in Table 1. The mean tumor volume of the 14 patients included in this study was ~24 cm^3 (range, 4–55 cm^3).

PET/CT scanner

All scans were performed on a General Electric Discovery LS PET (Advance NXi)/CT (LightSpeed four-slice) scanner (GE HealthCare, Waukesha, WI). The LightSpeed CT has a 50-cm transaxial field of view, with a slice thickness of 0.63–20.0 mm. The tube current can be varied between 10 and 440 mA and the tube voltage between 80 and 140 kVp, in increments of 20 kVp.

The PET Advance NXi scanner is a whole body scanner with a transaxial and axial field of view of 55 and 15.2 cm, respectively. The scanner has septa for high-resolution two-dimensional image acquisition; the septa can be retracted for high-sensitivity three-dimensional imaging. In the present study, PET was done exclusively in the two-dimensional mode. The intrinsic resolution is 4.2 mm full-width at half maximum.

FMISO imaging protocol

The patients were injected intravenously with an average of 10.4 mCi (range, 9.3–11) of FMISO. No fasting period before the FMISO injection was required.

The patients were scanned in the supine position on a flat-top couch insert. The head, neck, and shoulders were immobilized using an Aquaplast mask prepared during the RT simulation session. To minimize patient misalignment during the multiple studies, marks were drawn on the flat insert to ensure proper repositioning of the immobilization hardware. In addition, small CT markers were used on the patient's immobilization mask to assist in the image registration.

Positron emission tomography data were acquired at a mean post-injection time of 162 min (maximum, 195 and minimum, 117) and 162 min (maximum, 195 and minimum, 126) for the first (FMISO1) and second (FMISO2) FMISO scans, respectively. Each of the FMISO studies covered two PET axial fields of view, with 8 min/field of view. FMISO emission data were corrected for attenuation, scatter, and randoms, and then iteratively reconstructed using the standard FDG reconstruction parameters used clinically (28 subsets, two iterations, postfilter, 6.0 mm full-width at half maximum, loop filter, 4.3 mm full-width at half maximum).

Venous blood samples were obtained immediately before and after the FMISO PET/CT session. The measured aliquots of each blood sample were counted in triplicate using a CompuGamma CS Gamma Counter (LKB-Wallac, Turku, Finland), and the net count rates were converted to activity concentrations (becquerels per cubic centimeter), and then decay corrected to the time of injection. Blood count data were converted into standardized uptake value (SUV) units.

Image analysis

All image registration among the two FMISO scans and with the FDG scan were performed using in-house image registration software, ImgReg (30,31), and was determined using mutual information between the CT image sets of the respective PET/CT examinations. The following procedure was used for all 14 patients. The FMISO1 study was considered the reference data set. The first step of the image registration involved manually aligning the different CT data sets, using the fiducial markers in the immobilization mask. The target volumes in the FDG-CT and CT-FMISO2 image sets were then registered rigidly to that in the CT-FMISO1 image set by maximizing the mutual information in the respective data sets. A sample example of the accuracy of the CT2-to-CT1 registration is shown in Fig. 1. The transformation matrices were then applied to the FDG and FMISO2 image sets, thus registering the FDG and FMISO2 target volumes to the FMISO1 target volume.

The imaging data initially available in units of microcuries per milliliter per voxel were decay corrected to the time of injection and converted into SUV units. The target volume (TV) was then segmented according to the FDG-PET/CT images. The FDG TV was defined using the iterative segmentation technique of Nehmeh *et al.* (32). The FDG-PET/CT TVs were then measured. The coordinates and SUV of each pixel in the corresponding volumes in the FMISO1 and FMISO2 images were then extracted to output files using ImageJ software (33).

Statistical analysis

For the convenience of presenting T/B threshold ratios for hypoxia tracer uptake, all values were converted to SUVs. The blood SUVs were determined using the measured blood aliquots per unit weight acquired at the PET scan, with decay corrected to the time of injection, divided by the administered activity per unit body weight.

The relationship between the FMISO1 and FMISO2 distributions within the TV was analyzed using a voxel-by-voxel SUV correlation between the registered tumor volumes. The corresponding Pearson correlation coefficient (R) was calculated using two criteria: *(1)* for all the voxels included within the TV; and *(2)* for all the voxels contained within the TV with a SUV greater than or equal to a T/B ratio of 1.2 for each of the two FMISO image sets. The goodness of the correlation between the FMISO1 and FMISO2 distributions was defined according to the following criteria: $R < 0.5$ indicates a weak correlation and $R \geq 0.5$, a strong correlation.

The scatter gram of FMISO1 vs. FMISO2 allowed the data to be partitioned into different quadrants: *(1)* if a voxel exceeded the 1.2 threshold in both FMISO1 and FMISO2, it would be in the upper right quadrant, perhaps indicative of chronic hypoxia; *(2)* if a voxel was less than the 1.2 threshold in both scans, it would be in the lower left quadrant and assumed to be normoxic; and *(3)* if the threshold value was exceeded by a voxel in either of the two FMISO studies, it would be in the upper left or lower right quadrant, perhaps indicating a change in the hypoxic status between the scans or suggestive of the influence of intermittent or acute hypoxia.

The fractional hypoxic volume (FHV), using a T/B ratio of 1.2, was defined as

$$FHV = \frac{FMISO\_TV_{T/B=1.2}}{FDG\_TV}$$

where the tumor volume (in the denominator) is defined by the viable tumor volume that shows FDG uptake.

Results

Figure 2a,b summarizes the blood SUV and maximal tumor SUV, respectively, measured in the two FMISO scans. The blood SUVs were similar in the studies for all patients, except for Patients 2 and 11, for which marked discrepancies in the ^{18}F-MISO activities were found. These values were the average of two blood samples, obtained immediately before and after the PET scan and reflect serum. Because both samples were consistent, we believe these differences were associated with genuine differences in blood clearance between the two scans. The FMISO tumor SUVs were within 20% for the two scans for all patients, except for Patient 2. In Fig. 3, the FHVs are presented for all the patients, with the hypoxic volume defined according to the number of voxels exceeding a threshold T/B ratio of ≥1.2 divided by the total number of voxels included in the tumor volume. For most patients, the hypoxic volumes derived from the two FMISO image sets were consistent. Four patients (Patients 3, 11, 12, and 13) had differences >20%.

Figure 4 presents the FMISO1 vs. FMISO2 scattergrams of the corresponding tumor voxel SUVs for all 14 patients. The scattergrams also show the threshold values defined by a T/B ratio ≥1.2, represented by the vertical (for FMISO1) and horizontal (for FMISO2) lines. The correlation coefficients (R) with and without the T/B threshold applied are summarized in Table 2. The gross tumor volume, maximal tumor SUV and maximal blood SUV scan time after injection, blood time after injection, and FHVs from the FMISO1 and FMISO2 scans are also summarized in Table 2. When no T/B threshold was applied, the average correlation coefficient between FMISO1 and FMISO2 was 0.6 (range, 0.3–0.8); 12 of 14 tumors showed a strong correlation. When the T/B ≥1.2 threshold was applied, the mean correlation coefficient between FMISO1 and FMISO2 decreased to 0.3 (range, 0–0.7); only 6 of 13 tumors showed strong correlation. The average FHV with the T/B ≥1.2 threshold applied was 44% (range, ~13% to ~100%) in FMISO1 and 41% (range, ~41 to ~82%) in FMISO2.

Our results also showed a strong correlation between the hypoxic volumes with the tumor volume. However, the hypoxic volume correlated strongly with the FMISO maximal SUV in both studies (R = ~0.8 and R = ~0.7 for FMISO1 and FMISO2, respectively; Fig. 4). No correlation could be established between the FMISO1-FMISO2 correlation, R, and the tumor volume, FHV, or SUV.

To show the large variability between the patients' repeat FMISO scans, we illustrated the diversity of behavior by showing images of the patient with the poorest correlation (Patient 6) and the best correlation (Patient 5) between FMISO1 and FMISO2 (Figs. 5 and 6).

Discussion

Hypoxia-induced radioresistance can be a significant cause of local tumor control failure after RT (34) owing to the increased radioresistance in hypoxic cells (35). This can be overcome by using IMRT to escalate the dose to hypoxic regions within tumors delineated on FMISO PET images. The determination of the reproducibility of FMISO-PET scans and an understanding of any intratumor distribution changes (if they occur) is a vital prerequisite to any proposal to incorporate such images into the RT planning process. The present study explicitly set out to

determine the degree of variation in the FMISO hypoxia-targeting tracer using a voxel-by-voxel analysis of the tracer distribution in repeat studies. The selection of a 3-day interval between FMISO scans was determined from the estimated time from treatment simulation, plan completion, and a patient undergoing the first RT fraction. Thus, changes between the FMISO1 and FMISO2 scans would reflect changes in the hypoxia distribution from that at the PET/CT simulation, the data used for IMRT planning, and the distribution at delivery of the first planned RT fraction.

In this study, we adopted the criterion suggested by Rajendran *et al.* (19) of a T/B ratio of ≥1.2 to delineate tumor hypoxia. Our results included an analysis of the voxel-by-voxel FMISO voxel uptake within the entire tumor volume from repeat PET studies, with and without applying a T/B threshold criterion. We found a strong correlation in 12 of 14 patients between the co-registered data sets when no threshold was used. However, for dose painting, one is primarily interested in the constancy of the relatively few most-intense voxels between the two FMISO scans. The inclusion of only hypoxic voxels (T/B ratio ≥1.2) in the correlation analysis reduced the correlation coefficient for all patients. Only 7 of 13 patients exhibited R values ≥0.5. This shows that most patients have some variation in the location of regional hypoxia as defined by FMISO PET scans. For example, Patient 11 demonstrated hypoxia in the entire TV in FMISO1, but only 44% of the TV fulfilled the criterion of a T/B ratio of ≥1.2 for FMISO2, resulting in a reduction in the correlation coefficient from 0.7 to 0.38 for this patient. This reduction in the correlation coefficient when analyzing PET images after the application of a threshold is a consequence of the contribution of what is frequently the majority of lower intensity (less than the threshold) voxels, which could remain well correlated even when a mismatch occurs in the location of the ^{18}F-FMISO hot spot on the respective FMISO1 and FMISO2 PET images. Also, several factors can reduce the quality of the correlation, including statistical noise. With voxel-by-voxel comparison of serial PET images of a phantom (data not shown), we have observed a correlation coefficient of only ~0.5. This spatial mismatch results from statistical variation, and it was from these phantom results that we established an R value of ≥0.5 as corresponding to “strong” correlation. Although attempts were made to minimize the PET scan times after injection, different setup times, and thus scan times, might have reduced the correlations between FMISO1 and FMISO2. The percentage of difference in tumor SUVs in FMISO1 and FMISO2 correlated well with the percentage of difference in time after injection between the two studies (R = ~0.5). This confirmed the behavior of the tumor uptake as a function of time after injection. However, no correlation could be established between similar measurements from the blood data, possibly because of the relatively slow blood clearance (*i.e.*, only 10% decrease in blood activity concentration 2–3 h after injection [36]). Inaccuracies in patient setup and consequent image registration based on mutual information of the CT component of the two FMISO1 and FMISO2 PET/CT examinations also affects the strength of the correlation. The error in patient setup has been estimated by Hong *et al.* (37) in head and neck cancer patients to be as much as 6.97 mm (*i.e.*, approximately two PET pixels).

Although our data have not proved the ability to use non-invasive PET imaging to identify regions of acute hypoxia, they do imply the presence of ongoing variations in tumor hypoxia and that each voxel could consist of a combination of acute and chronic hypoxia components (38). The size of each PET voxel (~4 × 4 × 4 mm) is much larger than a microenvironment region of tumor hypoxia, which has dimensions of ≤100 μm. Thus, each PET voxel might contain large numbers of microscopic regions of hypoxia detectable by immunohistochemical analysis of tumor biopsy specimens (7). Thus, the intensity of FMISO within any PET image voxel likely reflects the composite uptake of a spectrum of microscopic regions, ranging from well-perfused and normoxic to poorly perfused and hypoxic to nonperfused and anoxic.

The results we have presented are dependent on the choice of a T/B ratio of 1.2 to define regions of tumor hypoxia. This threshold value was first proposed by Rajendran *et al.* (19) from the

University of Washington, who have had the greatest experience with FMISO, using it to image a number of tumors, including head and neck cancer. This threshold was selected empirically based on the observation that >95% of normal tissue voxels in FMISO total body PET scans had a tissue/blood ratio of ≤1.2. Clearly, the selection of any single threshold value to identify hypoxic regions has limitations. For example, the use of a 1.2 threshold to delineate hypoxic volumes resulted in all tumor voxels of FMISO2 in Patient 2 being highlighted for the second FMISO2 scan, yielding a FHV of nearly 100%.

Furthermore, we observed that small changes in the threshold level could have a considerable effect on the FMISO1 vs. FMISO2 correlation. For example, for Patient 5, a T/B ratio of 1.2, 1.3, and 1.4 resulted in widely different correlation coefficients (R = 0.7, R = 0.8, and R = 0.3, respectively). Thus, we included the R values for data with and without the threshold (T/B ratio ≥1.2) in Table 2. We also investigated the selection of an alternative to blood for the comparison with tumor, because it was shown for Patients 2 and 11 that significant variations can occur in the blood SUV. This variation could not be accounted for by differences in injected ^{18} F-MISO activity or the blood sample time after injection. Therefore, the tumor/muscle activity concentration ratio was also evaluated. However, for our patient cohort, we found no improvement in the reproducibility of FMISO-based FHVs in the tumor (data not shown).

Conclusion

The results of this preliminary study have shown the considerable variability in the intratumor uptake that can occur between repeat ^{18}F-FMISO PET scans performed 3 days apart in patients with head-and-neck cancer. Only 6 of 13 patients had a strong voxel-by-voxel correlation suggestive of a reasonably stable radiotracer distribution and chronic hypoxia. The other 7 patients exhibited variable degrees of mismatch between the location of the most intense areas within the tumor between FMISO1 and FMISO2. These findings suggest that additional work is required to identify the underlying causes of changes in intratumor radiotracer distribution before ^{18}F-FMISO PET images can be used as the basis of hypoxia-targeting IMRT planning. Only then, could ^{18}F-FMISO PET/CT-guided dose painting IMRT be used to dose escalate the hypoxic gross tumor volume within the tumor volume (without compromising normal tissue sparing) and thus reducing gross tumor volume radiation resistance due to hypoxia and improving local control.

Acknowledgments

This study was funded by the ASTRO Junior Investigator Award.

References

1. Dubois L, Landuyt W, Haustermans K, et al. Evaluation of hypoxia in an experimental rat tumour model by [(18)F]fluoromisonidazole PET and immunohistochemistry. Br J Cancer 2004;91:1947–1954. [PubMed: 15520822]
2. Chapman JD. The detection and measurement of hypoxic cells in solid tumors. Cancer 2006;54:2441–2449. [PubMed: 6333921]
3. Vaupel P, Kallinowski F, Ohunieff P. Blood flow, oxygen and nutrient supply, and metabolic micro-environment of human tumors: Review. Cancer Res 1989;49:6449–6465. [PubMed: 2684393]
4. Brizel DM, Rosner GL, Harrelson J, et al. Pretreatment oxygenation profiles of human soft tissue sarcomas. Int J Radiat Oncol Biol Phys 1994;30:635–642. [PubMed: 7928495]
5. Nordsmark M, Bentzen SM, Rudat V. Prognostic value of tumor oxygenation in 397 head and neck tumors after primary radiation therapy: An international multi-center study. Radiother Oncol 2005;77:18–24. [PubMed: 16098619]
6. Koukourakis MI, Bentzen SM, Giatromanolaki A, et al. Endogenous markers of two separate hypoxia response pathways (hypoxia inducible factor 2 alpha and carbonic anhydrase 9) are associated with

radiotherapy failure in head and neck cancer patients recruited in the CHART randomized trial. J Clin Oncol 2006;24:727–735. [PubMed: 16418497]

7. Bussink J, Kaanders JH, van der Kogel AJ. Tumor hypoxia at the micro-regional level: Clinical relevance and predictive value of exogenous and endogenous hypoxic cell markers. Radiother Oncol 2003;67:3–15. [PubMed: 12758235]
8. Rasey JS, Hofstrand PD, Chin LK, et al. Characterization of [18F]fluoroetanidazole, a new radiopharmaceutical for detecting tumor hypoxia. J Nucl Med 1999;40:1072–1079. [PubMed: 10452326]
9. Nordsmark M, Loncaster J, Chou SC, et al. Invasive oxygen measurements and pimonidazole labeling in human cervix carcinoma. Int J Radiat Oncol Biol Phys 2001;49:581–586. [PubMed: 11173158]
10. Fyles A, Milosevic M, Hedley D, et al. Tumor hypoxia has independent predictor impact only in patients with node-negative cervix cancer. J Clin Oncol 2002;20:680–687. [PubMed: 11821448]
11. Hoeckel M, Knoop C, Schlenger B, et al. Intratumoral pO_2 predicts survival in advanced cancer of the uterine cervix. Radiother Oncol 1993;26:45–50. [PubMed: 8438086]
12. Knowles HJ, Phillips RM. Identification of differentially expressed genes in experimental models of the tumor microenvironment using differential display. Anticancer Res 2001;21:2305–2311. [PubMed: 11724287]
13. Mankoff DA, Dunnwald LK, Gralow JR, et al. Blood flow and metabolism in locally advanced breast cancer: Relationship to response to therapy. J Nucl Med 2002;43:500–509. [PubMed: 11937594]
14. Valk P, Mathis C, Prados M, et al. Hypoxia in human gliomas: Demonstration by PET with flouorine-18-fluoromisonidazole. J Nucl Med 1992;33:2133–2137. [PubMed: 1334136]
15. Hockel M, Schlenger K, Arad D, et al. Association between tumor hypoxia and malignant progression in advanced cancer of the uterine cervix. Cancer Res 1996;56:4509–4515. [PubMed: 8813149]
16. Adam M, Gabalski EC, Bloch DA, et al. Tissue oxygen distribution in head and neck cancer patients. Head Neck 1999;21:146–153. [PubMed: 10091983]
17. Brizel DM, Sibley GS, Prosnitz LR, et al. Tumor hypoxia adversely affects the prognosis of carcinoma of the head and neck. Int J Radiat Oncol Biol Phys 1997;38:285–289. [PubMed: 9226314]
18. Rajendran JG, Mankoff DA, O'Sullivan F, et al. Hypoxia glucose metabolism in malignant tumors: Evaluation by [18F]fluoromisonidazole and [18F]fluorodeoxyglucose positron emission tomography imaging. Clin Cancer Res 2004;10:2245–2252. [PubMed: 15073099]
19. Rajendran JG, Wilson DC, Conrad EU. [(18)F]FMISO and [(18)F]FDG PET imaging in soft tissue sarcomas: Correlation of hypoxia, metabolism and VEGF expression. Eur J Nucl Med Mol Imaging 2003;30:695–704. Epub 2003 Mar. [PubMed: 12632200]
20. Rasey JS, Koh WJ, Evans ML, et al. Quantifying regional hypoxia in human tumors with positron emission tomography of [18F]fluoromisonidazole: A pretherapy study of 37 patients. Int J Radiat Oncol Biol Phys 1996;36:417–428. [PubMed: 8892467]
21. Gagel B, Reinartz P, Dimartino E, et al. pO(2) Polarography versus positron emission tomography ([(18)F] fluoromisonidazole, [(18)F]-2-fluoro-2′-deoxyglucose): An appraisal of radiotherapeutically relevant hypoxia. Strahlenther Onkol 2004;180:616–622. [PubMed: 15480509]
22. Eschmann SM, Paulsen F, Reimold M, et al. Prognostic impact of hypoxia imaging with 18F-misonidazole PET in non-small cell lung cancer and head and neck cancer before radiotherapy. J Nucl Med 2005;46:253–260. [PubMed: 15695784]
23. Koh WJ, Bergman KS, Rasey JS, et al. Evaluation of oxygenation status during fractionated radiotherapy in human nonsmall cell lung cancers using [F-18]fluoromisonidazole positron emission tomography. Int J Radiat Oncol Biol Phys 1995;33:391–398. [PubMed: 7673026]
24. Casciari JJ, Graham MM, Rasey JS. A modeling approach for quantifying tumor hypoxia with [F-18] fluoromisonidazole PET time-activity data. Med Phys 1995;22:1127–1139. [PubMed: 7565388]
25. Rajendran JG, Krohn KA. Imaging hypoxia and angiogenesis in tumors. Radiol Clin North Am 2005;43:169–187. [PubMed: 15693655]
26. Overgaard J, Horsman MR. Modification of hypoxia-induced radioresistance in tumors by the use of oxygen and sensitizers. Semin Radiat Oncol 1996;6:10–21. [PubMed: 10717158]
27. Evans SM, Koch CJ. Prognostic significance of tumor oxygenation in humans. Cancer Lett 2003;195:1–16. [PubMed: 12767506]

28. Ling CC, Humm J, Larson S, et al. Towards multidimensional radiotherapy (MD-CRT): Biological imaging and biological conformality. Int J Radiat Oncol Biol Phys 2000;47:551–560. [PubMed: 10837935]
29. Chao KS, Bosch WR, Mutic S, et al. A novel approach to overcome hypoxic tumor resistance: Cu-ATSM-guided intensity-modulated radiation therapy. Int J Radiat Oncol Biol Phys 2001;49:1171–1182. [PubMed: 11240261]
30. Hu Y, Erdi A, Chui C. A 3-D image registration toolkit for radiation therapy treatment planning [Abstract]. Med Phys 1999;26:1160.
31. Erdi AK, Hu YC, Chui CS. Using mutual information (MI) for automated 3D registration in the pelvis and thorax region for radiotherapy treatment planning. Proc SPIE Med Imaging 2000;3979:416–425.
32. Nehmeh, S.; El-Zeftawy, H.; Erdi, Y., et al. An iterative technique for lesion segmentation in PET images [Abstract]; J Nucl Med. 2006. p. 364Accessed at www.graylab.ac.uk/lab/reviews/hypoxia/html
33. ImageJ. [June 2006]. Available from: http://rsb.info.nih.gov/ij
34. HodgKiss RJ. Predictive assays for tumour hypoxia: Where are we going? Gray Laboratory Annual Report. 1993
35. Hall, EJ. Radiobiology for the radiologist. 6th. Philadelphia: Lippincott Williams&Wilkins;; 2005.
36. Garrecht BM, Chapman JD. The labelling of EMT-6 tumours in BALB/C mice with 14C-misonidazole. Br J Radiol 1983;56:745–753. [PubMed: 6616139]
37. Hong T, Tomé W, Chappell R, et al. The impact of daily setup variations on head-and-neck intensity-modulated radiation therapy. Int J Radiat Oncol Biol Phys 2005;61:779–788. [PubMed: 15708257]
38. Wang K, Yorke ED, Nehmeh SA, et al. Analyzing serial hypoxia images from ^{18}FMISO-PET: Modeling transient and chronic hypoxia [Abstract]. Int J Radiat Oncol Biol Phys 2006;66(Suppl):S3.

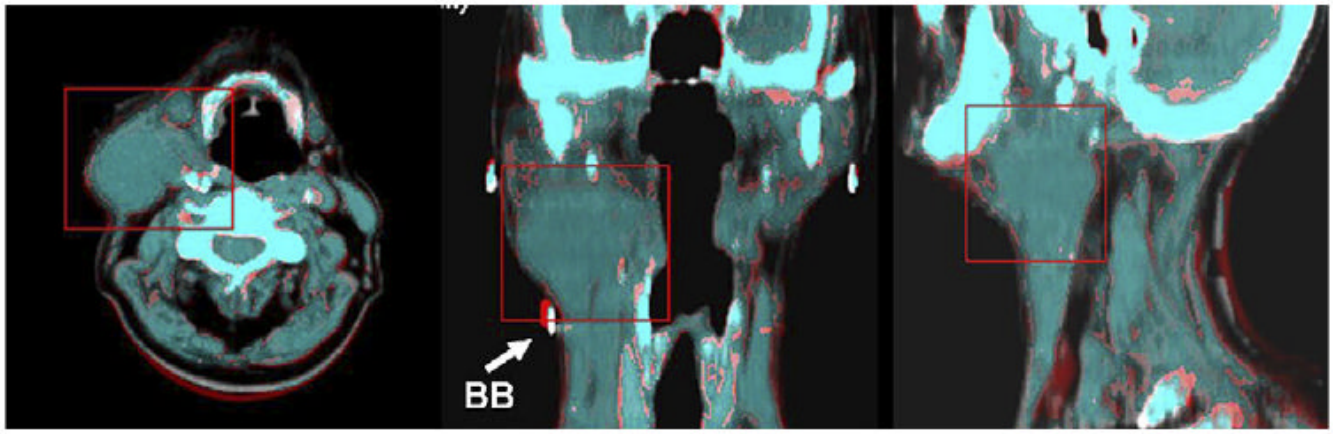

Fig. 1.
Transaxial, coronal, and sagittal views depicting accuracy of computed tomography (CT)1-to-CT2 registration. Red box corresponds to registered volume. Coronal view shows one of the BBs used to assist in registration (BB diameter, 1 mm).

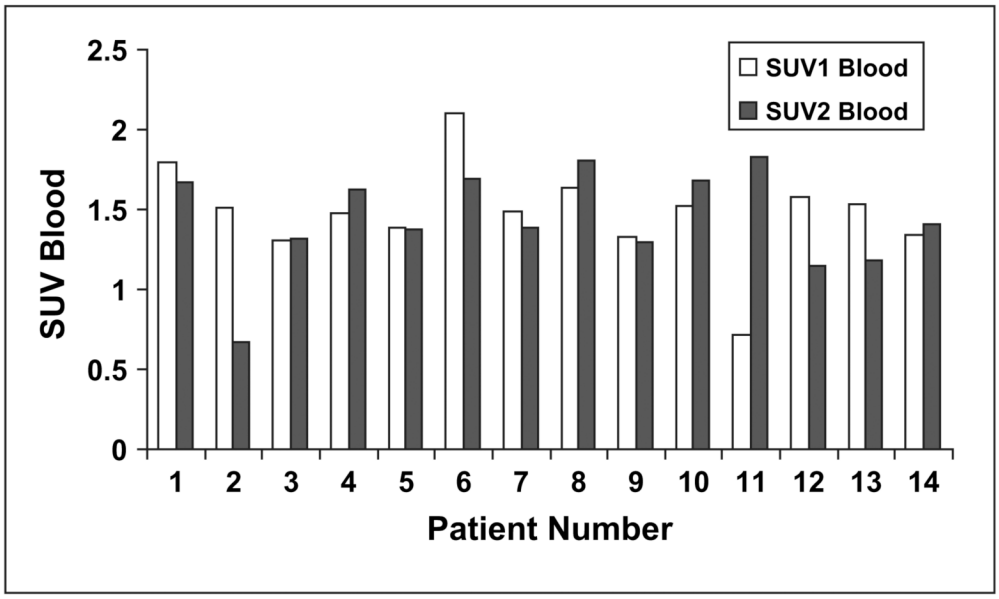

(a)

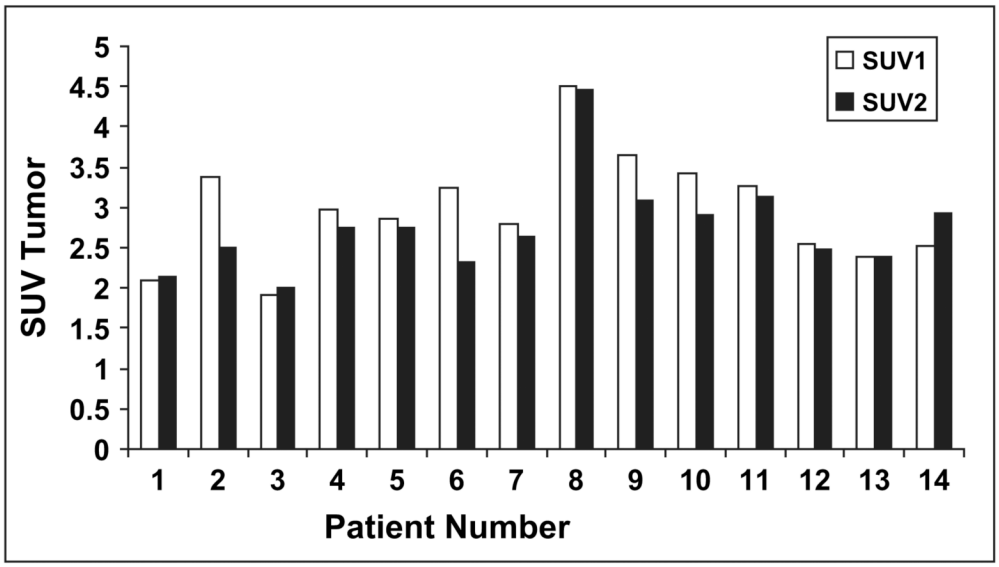

(b)

Fig. 2.
(a) Blood and (b) tumor standardized uptake values (SUVs) measured in ^{18}F-fluoromisonidazole (FMISO)1 and FMISO2.

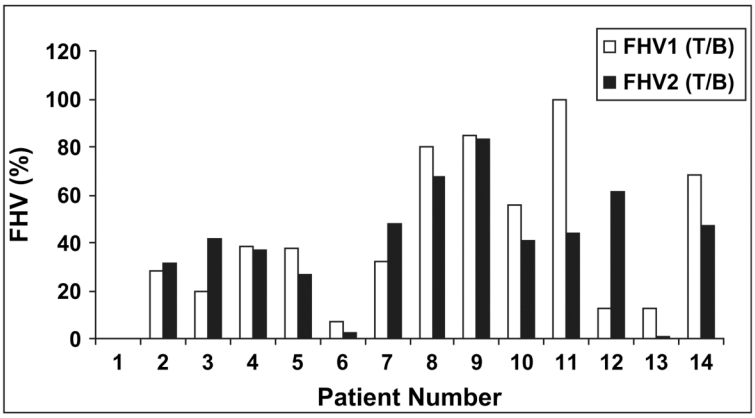

Fig. 3.

Fractional hypoxic volumes (FHV), defined as the hypoxic volume (using a tumor/blood [T/B] threshold ≥1.2) divided by target volume.

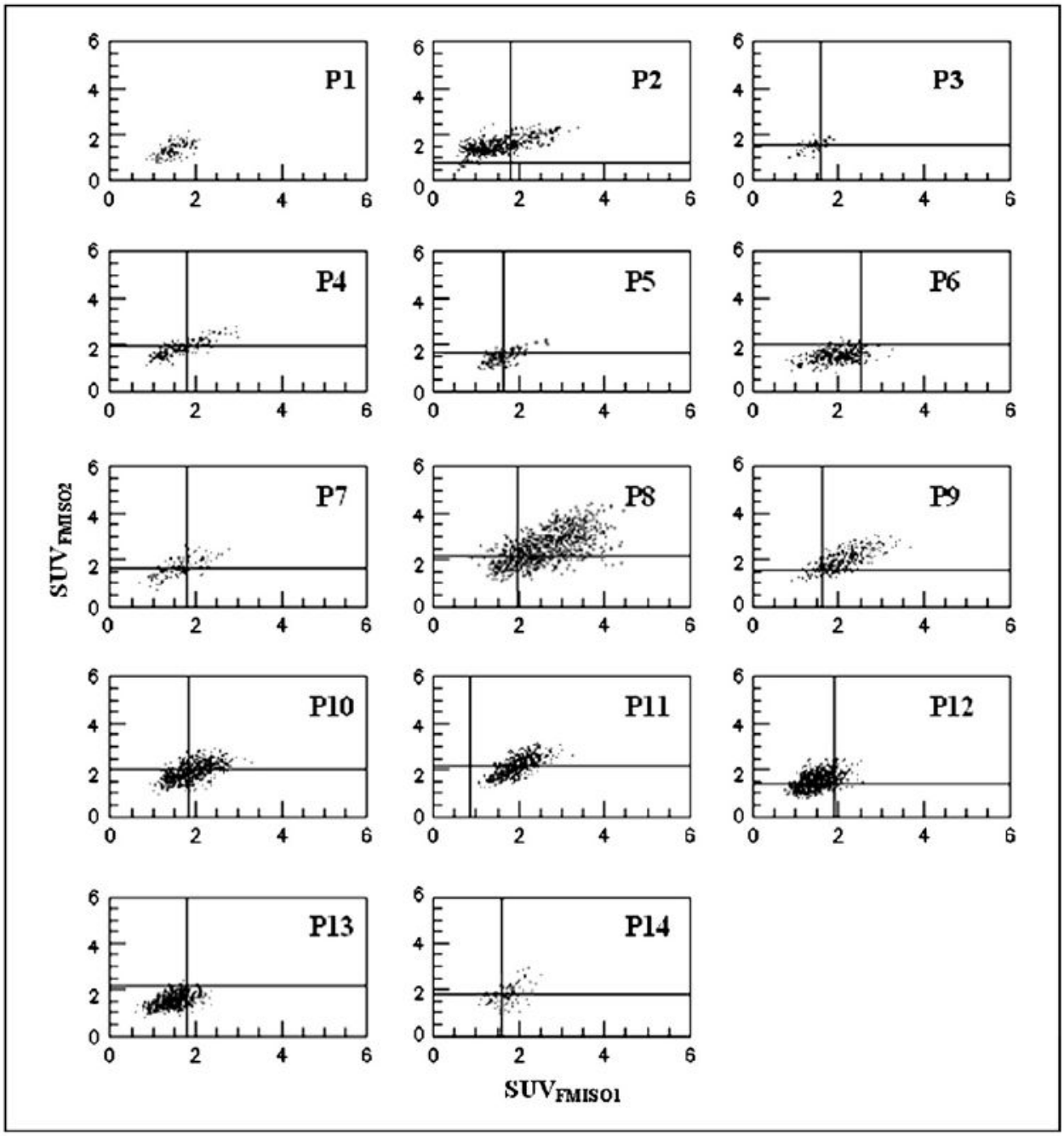

Fig. 4.

Scattergrams representing pair wise standardized uptake value (SUV) voxel values within target volume for ^{18}F-fluoromisonidazole (FMISO)1 and FMISO2. In each panel, tumor/blood ratio of 1.2 presented by vertical (FMISO1) and horizontal (FMISO2) lines. No threshold could be established for Patient 1 (P1) because of technical problems with blood sample.

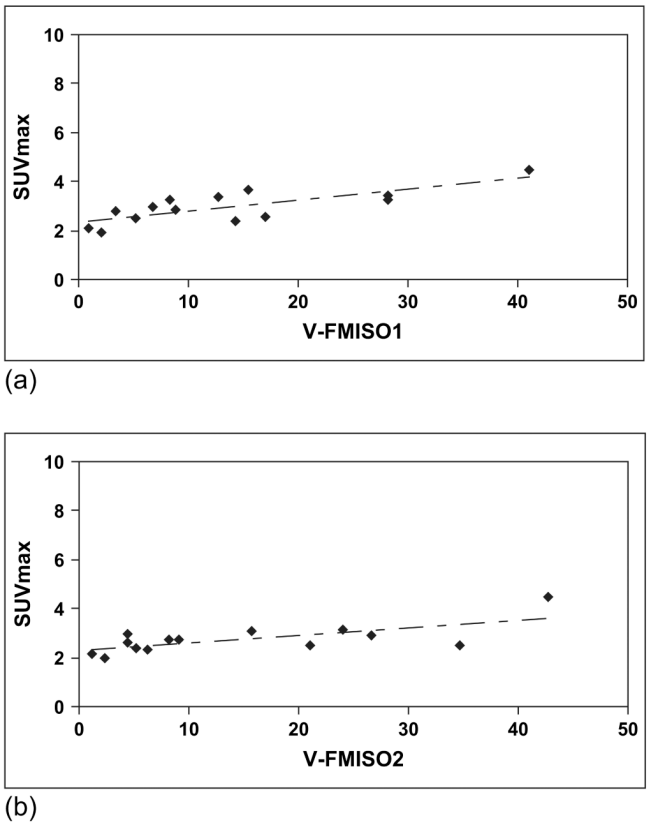

Fig. 5.

Maximal standardized uptake value (SUV_{max}) for tumor vs. hypoxic volume (using tumor/blood threshold of ≥1.2) for (a) ^{18}F-fluoromisonidazole (FMISO)1 and (b) FMISO2 studies.

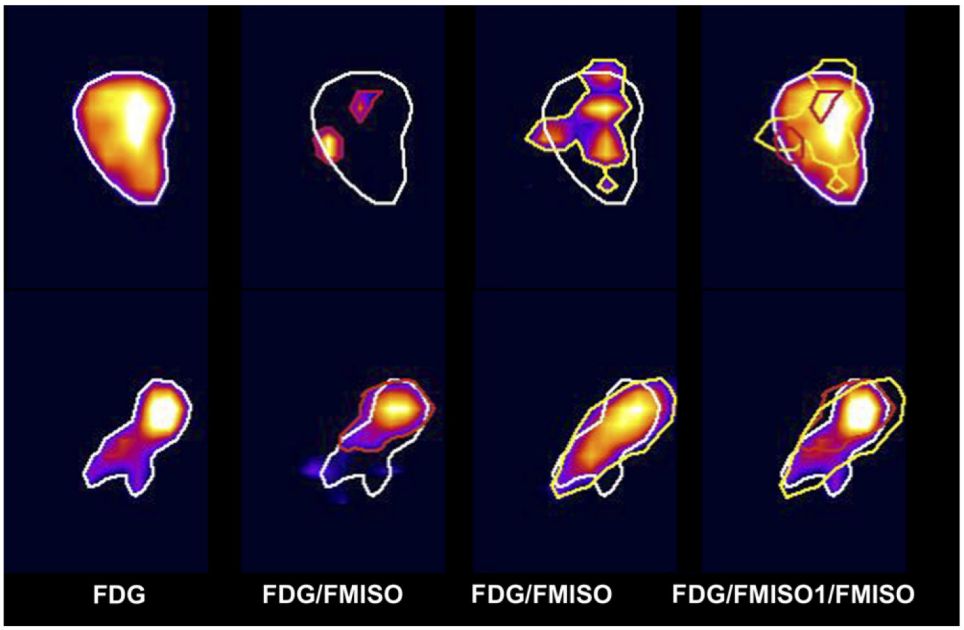

Fig. 6.

Transaxial, coronal, and sagittal views of fluorodeoxyglucose (FDG) target volume (TV), and hypoxic volumes in ^{18}F-fluoromisonidazole (FMISO)1 and FMISO2 as defined by tumor/blood (TB) ratio of ≥1.2. Large variability between patients' repeat FMISO scans illustrated for patient with poorest (Patient 6, Top) and best (Patient 5, Bottom) correlation between FMISO1 and FMISO2. Images show transaxial, coronal, and sagittal views.

Table 1

Patient characteristics

Pt. no.	Primary disease	Stage	Age (y)
1	BOT	III	79
2	BOT	IVA	67
3	Oropharynx	III	48
4	Larynx	III	68
5	Larynx	IVA	54
6	BOT	IVA	62
7	Oropharynx	IVA	60
8	Oropharynx	IVA	64
9	BOT	IVA	55
10	Oropharynx	IVA	60
11	Oropharynx	III	62
12	BOT	IVB	66
13	Oropharynx	IVA	56
14	Oropharynx	IVA	47

Abbreviations: Pt. no. = patient number; BOT = base of tongue.

Int J Radiat Oncol Biol Phys. Author manuscript; available in PMC 2010 March 12.

Table 2

Tumor GTV, maximal tumor SUV, maximal blood SUV scan time after injection, blood time after injection, FHVs, and correlation coefficients, R, between corresponding voxel SUVs within TV of aligned FMISO1 FMISO2 TVs

				Scan time PI (min)		Blood time PI (min)		T/B ratio		R value*	
Pt. no.	**$SUV_{max-FDG}$**	**$SUV_{max-FMISO1}$**	**$SUV_{max-FMISO2}$**	**FMISO1**	**FMISO2**	**FMISO1**	**FMISO2**	**FHV1**	**FHV2**	**All**	**T/B ≥ 1.2**
1	10.5	2.1	2.1	171.0	172.0	176.0	168.0	16.6	19.8	0.6	N/A
2	9.8	3.4	2.5	192.0	148.0	186.0	126.0	60.3	99.7	0.6	0.5
3	14.8	1.9	2.0	180.0	142.0	169.0	120.0	74.4	83.7	0.7	0.3
4	17.5	3.0	2.8	150.0	126.0	140.0	142.0	66.0	79.2	0.8	0.7
5	7.3	2.9	2.8	155.0	176.0	145.2	148.8	43.3	44.9	0.7	0.7
6	25.8	3.2	2.3	147.0	146.0	139.8	145.8	36.0	26.8	0.3	0.0
7	7.8	2.8	2.6	152.0	161.0	129.0	140.0	69.7	89.5	0.7	0.1
8	12.3	4.5	4.4	166.0	195.0	151.0	141.0	93.8	97.8	0.6	0.5
9	136.6	3.7	3.1	180.0	164.0	141.0	145.0	98.4	99.5	0.7	0.7
10	11.5	3.4	2.9	195.0	170.0	175.0	145.0	87.7	82.8	0.6	0.1
11	17.3	3.3	3.1	114.0	133.0	117.0	113.0	100.0	85.1	0.7	0.4
12	9.3	2.5	2.5	155.0	192.0	137.0	150.0	44.4	90.4	0.5	0.0
13	16.3	2.4	2.4	157.0	150.0	140.0	95.0	45.0	16.3	0.5	0.0
14	105.0	2.5	2.9	153.0	187.0	140.0	185.0	89.0	74.7	0.4	0.5
Maximum	136.6	4.5	4.4	195.0	195.0	186.0	185.0	100.0	99.7	0.8	0.7
Minimum	7.3	1.9	2.0	114.0	126.0	117.0	95.0	16.5	16.3	0.3	0.0
Average	34.1	3.0	2.8	161.0	161.4	149.3	140.3	65.1	69.1	0.6	0.3

Abbreviations: GTV = gross tumor volume; SUV = standardized uptake value; FHV = fractional hypoxic volume; TV = target volume; FMISO1 = ^{18}F-fluromisonidazole scan on Day 1; FMISO2 = FMISO scan on Day 4; Pt. no. = patient number; $SUV_{max-FDG}$ = flurodeoxyglucose maximal SUV; T/B = tumor/blood ratio.

* R values calculated for all voxels within TV and for those within TV and satisfying T/B ratio ≥1.2 threshold. No blood data were available for Patient 1; thus, R value for T/B ratio ≥1.2 not applicable.